IOPscience iopscience.iop.org

Home Search Collections Journals About Contact us My IOPscience

Kinetic analysis of the collisional plasma–sheath transition

This content has been downloaded from IOPscience. Please scroll down to see the full text.

2003 J. Phys. D: Appl. Phys. 36 2811

(http://iopscience.iop.org/0022-3727/36/22/007)

View the table of contents for this issue, or go to the journal homepage for more

Download details:

IP Address: 136.206.1.12
This content was downloaded on 03/05/2015 at 16:30

Please note that terms and conditions apply.

INSTITUTE OF PHYSICS PUBLISHING JOURNAL OF PHYSICS D: APPLIED PHYSICS

J. Phys. D: Appl. Phys. **36** (2003) 2811–2820 PII: S0022-3727(03)60297-4

Kinetic analysis of the collisional plasma–sheath transition

K-U Riemann

Institut für Theoretische Physik, Ruhr-Universität Bochum, D-44780 Bochum, Germany

Received 4 March 2003
Published 30 October 2003
Online at stacks.iop.org/JPhysD/36/2811

Abstract
The subdivision of the plasma boundary layer into a quasi-neutral presheath and a collision-free sheath is strictly valid only in the asymptotic limit $\lambda_D/\lambda \to 0$, where λ_D is the electron Debye length and λ the ion mean free path. This trivial fact requires one to discuss the applicability and correct interpretation of the plasma–sheath concept for finite ratios λ_D/λ. In a former fluid analysis (Riemann K-U 1997 *Phys. Plasmas* **4** 4158) based on the charge exchange model the plasma–sheath transition was investigated on an intermediate scale. The analysis showed that there is no need and no justification for a modification of the Bohm criterion for finite λ_D. The former results and conclusions are confirmed and improved by a new kinetic analysis. The kinetic analysis of the plasma–sheath transition can be generalized to other presheath mechanisms.

1. Introduction

Nearly from the beginning, the pioneers of gaseous electronics distinguished the extended plasma bulk and a thin sheath separating the plasma from limiting walls [1]. This distinction is based on the following simple picture of the plasma–wall interaction. The plasma, as a highly conducting medium, is more or less free of space charges ('quasi-neutral') and sustains only weak electric fields. If the plasma is in contact with a material wall, charged particles hitting the wall are absorbed (or neutralized) there. Due to the high electron mobility, the wall is usually negatively charged. As a consequence, the major part of the electron population is repelled in front of the wall, and a thin positive space charge layer—the 'sheath'—is formed. The sheath has an extension of some (say ten) electron Debye lengths λ_D and shields the quasi-neutral plasma from the field produced by the surface charge at the wall.

Actually, however, the formation of a positive sheath is impeded by ion losses to the wall. In the case of a thin collisionless sheath this difficulty leads to the famous Bohm criterion [2]. (Bohm's formulation 'a criterion for a stable sheath' is somewhat misleading. Actually, it is a necessary condition for the shielding by a stationary sheath.) In the most simple case of a monoenergetic ion flow, the Bohm criterion requires that the ions enter the sheath region at least with ion sound velocity,

$$v_i \geqslant c_s = \sqrt{\frac{\kappa T_e}{m_i}}, \tag{1}$$

where κ is Boltzmann's constant, T_e denotes the electron temperature, and m_i is the ion mass. Under usual discharge conditions ('cold' ions, ion temperature $T_i < T_e$) this condition cannot be satisfied by the thermal motion of the ions leaving the plasma volume. Consequently, the shielding cannot be perfect, and a residual electric field penetrates into the quasi-neutral plasma and accelerates the ions. The region, where this acceleration takes place (depending on the special conditions it may be an additional layer or the whole plasma), is called the 'presheath'. Its typical extension L (in this paper, the ion mean free path λ) is large compared with the Debye length λ_D. We thus come to the following crude picture of the plasma–sheath transition (see figure 1; for a more detailed discussion and justification we refer to the review papers [3, 4]).

For small but finite ratios λ_D/L (figure 1(*a*)) the electric potential Φ shows a steep gradient ($e\,\mathrm{d}\Phi/\mathrm{d}z \sim \kappa T_e/\lambda_D$) in the sheath, and a weak gradient ($e\,\mathrm{d}\Phi/\mathrm{d}z \sim \kappa T_e/L$) in the presheath. In the limiting case $\lambda_D/L \to 0$, we must distinguish the separate scales $x = z/L$ of the presheath (figure 1(*b*)) and $\xi = z/\lambda_D$ of the sheath (figure 1(*c*)).

On the presheath scale ($z = \mathrm{O}(L)$ or $x = \mathrm{O}(1)$) the sheath ($z = \mathrm{O}(\lambda_D)$ or $x = \mathrm{O}(\varepsilon) \to 0$) is infinitely thin. Correspondingly, the sheath potential becomes infinitely steep and is represented by the vertical line $x = 0$ in figure 1(*b*). The transition to this infinitely steep variation is (usually) indicated by a field singularity $\mathrm{d}\Phi/\mathrm{d}x \to -\infty$ of the presheath solution. In a simple fluid picture this singularity may be interpreted by the ion sound barrier [5]. It characterizes the 'sheath edge' and

 © 2003 IOP Publishing Ltd Printed in the UK

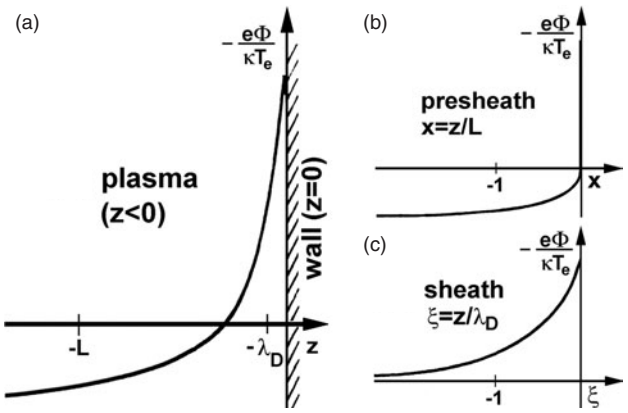

Figure 1. Schematic potential variation in the plasma ($z < 0$) in front of a negative absorbing wall ($z = 0$). (*a*) λ_D/L small but finite; (*b*) $\lambda_D/L \to 0$, presheath scale $x = z/L$; (*c*) $\lambda_D/L \to 0$, sheath scale $\xi = z/\lambda_D$.

is related to the marginal validity (equality form) of the Bohm criterion.

Resolving, on the other hand, the sheath potential variation on its natural scale $z = \mathrm{O}(\lambda_D)$ or $\xi = \mathrm{O}(1)$, the presheath ($z = \mathrm{O}(L)$ or $\xi = \mathrm{O}(1/\varepsilon) \to \infty$) appears infinitely remote, and the sheath edge is defined by a fading field ($\mathrm{d}\Phi/\mathrm{d}\xi \to 0$ for $\xi \to -\infty$) on the sheath scale.

The different asymptotic field limits

$$\begin{aligned} \frac{\mathrm{d}\Phi}{\mathrm{d}x} &\to -\infty \qquad (x \to 0), \\ \frac{\mathrm{d}\Phi}{\mathrm{d}\xi} &\to 0 \qquad (\xi \to -\infty), \end{aligned} \tag{2}$$

characterizing the sheath edge were again and again misinterpreted and regarded as a lack or even contradiction of the plasma–sheath concept [6–11]. Simultaneously, the Bohm criterion, which is closely related to the sheath edge singularity, was doubted or modified. Corresponding attempts to 'improve' the Bohm criterion, however, are based on an arbitrary definition of the sheath edge which are not consistent with the two scale concept [3, 12, 13].

Actually, the plasma–sheath concept sketched above is strictly valid only in the asymptotic limit $\varepsilon = \lambda_D/L \to 0$. For practical applications, it is therefore important to judge the significance of the asymptotic concept for small but finite values ε and to interpret it correctly. Due to the sheath edge singularity smooth matching of the presheath- and sheath profiles is not possible—and this holds even for arbitrarily small values of ε!

To answer the question of the significance of the asymptotic concept for finite λ_D/L and to remove the matching difficulty, it is necessary to investigate the vicinity of the sheath edge on an intermediate scale ℓ_m that is large compared with the Debye length λ_D but small compared with the characteristic presheath length L. On this scale both space charges and presheath processes must be accounted for in lowest order. Corresponding fluid analyses were presented for special problems or models, e.g. [14, 15] (probe theory), [16, 17] (Tonks–Langmuir model of the collisionless plasma column) and [18] (collisional presheath). All these fluid models resulted in the same characteristic extension $\ell_m = \lambda_D^{4/5} L^{1/5}$ of the intermediate scale, and it can indeed be shown [4] that there is one universal intermediate solution for all fluid models.

This universal solution, however, is not consistent with a kinetic analysis of the plasma–sheath transition. The difference is caused by the crucial space charge contribution of slow ions that cannot be adequately described in fluid theory. Franklin and Ockendon [16] showed that the intermediate scale of the kinetic Tonks–Langmuir problem [1, 19] has a characteristic extension $\ell_m = \lambda_D^{8/9} L^{1/9}$, but they did not give an explicit solution. Riemann [20] found the same scaling for the cold charge exchange (CX) model of the collisional presheath and presented an approximate solution based on crude approximations. A rigorous kinetic analysis of the plasma–sheath transition is still missing until now. It is the aim of this (and a subsequent) paper to fill this gap.

To this end we refer to our kinetic charge model of the collisional presheath [21] and follow the arguments and ideas of the previous fluid analysis [18]. In section 2, we introduce the model assumptions and present the basic equations. The asymptotic ($\varepsilon = 0$) solution of the problem [21] is briefly recalled in section 3. On the basis of numerical solutions for various finite ε, we exhibit in section 4 the interpretation difficulties of the plasma–sheath concept and demonstrate the significance of the intermediate scale $\ell_m = \lambda_D^{8/9} L^{1/9}$. An analytical description of the intermediate scale follows in section 5. In section 6, we sketch the generalization to other presheath models, and section 7 deals with the significance of the Bohm criterion. The results and conclusions are finally summarized and discussed in section 8.

2. Model and basic equations

We consider a one-dimensional weakly ionized plasma in front of a plane absorbing wall. The wall position is given by $z = z_w$, and the plasma is characterized by $z < z_w$. The electric potential Φ is governed by Poisson's equation

$$e(n_i - n_e) = -\varepsilon_0 \frac{\mathrm{d}^2\Phi}{\mathrm{d}z^2}, \tag{3}$$

where $n_{i,e}$ denotes the density of (singly charged positive) ions and electrons. The wall is sufficiently negative, and the electrons are assumed to be in Boltzmann equilibrium

$$n_e = n_{\mathrm{ch}} \exp \frac{e\Phi}{\kappa T_e} \tag{4}$$

with a characteristic charged particle density n_{ch} and the electron temperature T_e. The ions are dominated by CX collisions with a cold neutral gas background, the mean free path λ is constant. Due to these assumptions, the ions can move only in the positive z-direction (i.e. field direction) and the ion velocity distribution function takes the one-dimensional form

$$F(z, \boldsymbol{v}) = \begin{cases} F(z, v_z)\delta(v_x)\delta(v_y) & (v_z \geqslant 0), \\ 0 & (v_z < 0). \end{cases} \tag{5}$$

Applying Holstein's CX model [22], the ion Boltzmann equation reads [21]

$$v_z \frac{\partial F}{\partial z} - \frac{e}{m_i} \frac{\mathrm{d}\Phi}{\mathrm{d}z} \frac{\partial F}{\partial v_z} = -\frac{v_z}{\lambda} F(z, v_z) + \frac{J_i}{\lambda} \delta(v_z). \tag{6}$$

Here, m_i is the ion mass and $J_i = \int v_z F(z, v_z) = \text{const.}$ denotes the ion current density.

For convenience, we introduce dimensionless quantities

$$\varphi = -\frac{e\Phi}{\kappa T_e}, \qquad y = \frac{m_i v_i^2}{2\kappa T_e},$$
$$x = k(\varphi) = \frac{z}{\lambda}, \qquad \varepsilon = \frac{\lambda_D}{\lambda} = \frac{1}{\lambda}\sqrt{\frac{\kappa T_e}{n_{\rm ch} e^2}}, \tag{7}$$

$$f(\varphi, y) = \frac{1}{n_{\rm ch}}\sqrt{\frac{\kappa T_e}{2m_i}} F(z, v_z), \qquad n(\varphi) = \frac{n_i}{n_{\rm ch}},$$
$$j = \frac{1}{n_{\rm ch}}\sqrt{\frac{\kappa T_e}{2m_i}} J_i. \tag{8}$$

In these variables, Boltzmann's equation (6) reads [21]

$$\frac{\partial f}{\partial \varphi} - \frac{\partial f}{\partial y} = k'(\varphi)\{j\delta(y) - f(\varphi, y)\}$$
$$\text{with } j = \int_0^\infty f(\varphi, y)\,\mathrm{d}y = \text{const.} \tag{9}$$

and Poisson's equation (3) takes the form

$$\varepsilon^2 \frac{\mathrm{d}^2\varphi}{\mathrm{d}x^2} = n - \mathrm{e}^{-\varphi} \qquad \text{with } n = \int_0^\infty y^{-1/2} f(\varphi, y)\,\mathrm{d}y. \tag{10}$$

Engaging Poisson's equation with the formal solution of the ion Boltzmann equation [21]

$$f(\varphi, y) = jk'(\varphi - y)\exp[k(\varphi - y) - k(\varphi)] \tag{11}$$

results in the integro-differential equation

$$\varepsilon^2 \frac{\mathrm{d}^2\varphi}{\mathrm{d}x^2} = -\varepsilon^2 \frac{k''(\varphi)}{k'^3(\varphi)} = j\int_{-\infty}^{\varphi} \frac{\mathrm{e}^{k(\eta)-k(\varphi)}}{\sqrt{\varphi - \eta}} k'(\eta)\,\mathrm{d}\eta - \mathrm{e}^{-\varphi} \tag{12}$$

to determine $k(\varphi)$. With $k(\varphi)$ both the self-consistent potential variation and the ion distribution function are known.

3. Asymptotic presheath- and sheath solutions

In the asymptotic case $\varepsilon = 0$ equation (12) can be solved analytically. Choosing the sheath edge to fix the coordinate origins $\varphi = 0$ and $x = 0$, we read from [21] the presheath solution

$$x = \begin{cases} k_0(\varphi) & \text{for } \varphi < 0, \\ 0 & \text{for } \varphi \geqslant 0 \end{cases} \tag{13}$$

with

$$k_0(\varphi) = \ln \frac{\Psi(\varphi + (1/2)\pi j^2)}{\Psi((1/2)\pi j^2)},$$
$$\Psi(t) = i\int_{\gamma - i\infty}^{\gamma + i\infty} \sqrt{\Gamma(s)}\mathrm{e}^{st}\,\mathrm{d}s \quad \text{and} \quad j = 0.881\,61. \tag{14}$$

The asymptotic solution (13) is plotted in figure 2(*a*). The potential has a logarithmic shape in the plasma region ($x \to -\infty$). Approaching the origin $\varphi = 0$, k_0 shows a parabolic shape

$$k_0(\varphi) = -a\varphi^2 + \mathrm{O}(\varphi^3) \qquad \text{with } a = 0.368\,43. \tag{15}$$

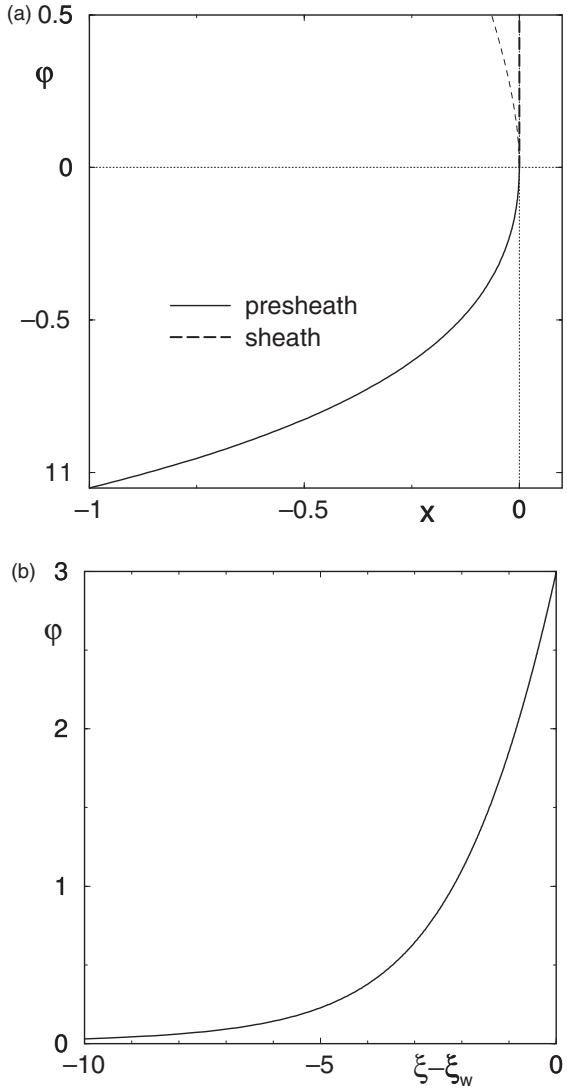

Figure 2. Asymptotic presheath- and sheath solutions for the CX-presheath model [21]: (*a*) presheath scale $x = z/\lambda$, (*b*) sheath scale $\xi = z/\lambda_D$. (The sheath solution refers to a wall potential $\varphi_w = 3$.)

At the vertex of the parabola the presheath solution ($\varphi < 0$) ends with a field singularity characterizing the sheath edge ($\varphi = 0$, $x = 0$). The continuation of $k_0(\varphi)$ beyond the vertex ($\varphi > 0$, thin dashed line in figure 2(*a*)) will be utilized in the analysis of section 5. It has, however, no physical significance. Instead, the asymptotic sheath potential $\varphi > 0$ is represented on the presheath scale by the degenerate solution $x = 0$.

To resolve the sheath potential, the problem must be re-considered on the sheath scale, where x is replaced by the space coordinate

$$\xi = \frac{z}{\lambda_D} = \frac{x}{\varepsilon}. \tag{16}$$

On this scale, Poisson's equation reads

$$\frac{\mathrm{d}^2\varphi}{\mathrm{d}\xi^2} = n - \mathrm{e}^{-\varphi} \tag{17}$$

and space charge can no longer be neglected for $\varepsilon \to 0$. On the other hand, the sheath is collisionless, because $k'(\varphi)$ in

equation (9) is replaced by $\varepsilon\, \mathrm{d}\xi/\mathrm{d}\varphi \to 0$ on the sheath scale. Consequently, the ion distribution function

$$f(\varphi, y) = f(0, y - \varphi) \tag{18}$$

in the sheath is explicitly known from the sheath edge ion distribution function $f(0, y)$. To calculate the sheath potential variation from Poisson's equation is therefore a simple integration task [21]. Figure 2(*b*) shows the result for a wall potential $\varphi_w = 3$. Approaching the sheath edge, it may be approximated in the form [21]

$$\xi = \text{const.} - 4.806\varphi^{-1/4}[1 + \mathrm{O}(\varphi^{1/2})] \qquad (\varphi \to 0). \tag{19}$$

In accord with the general discussion of section 1 (see equation (2)), it is quite obvious that the presheath solution (see figure 2(*a*)) and the sheath solution (see figure 2(*b*)) represent two completely different approaches that have no common range of validity and cannot be smoothly matched. The presheath solution is restricted to $\varphi < 0$ and runs into the singularity represented by the vertex of the parabola (15). The sheath solution, in contrast, is defined only for $\varphi > 0$ and tends asymptotically to a fading field described by equation (19).

4. Numerical results

For finite $\varepsilon = \lambda_D/\lambda > 0$ we solve equation (12) numerically. (The procedure is described in appendix A. For the solution of a similar problem with alternative techniques we refer to [23, 24].) In figure 3, we show the resulting potential profiles both on the presheath scale ($x = z/\lambda$, upper frame) and on the sheath scale ($\xi = z/\lambda_D = x/\varepsilon$, lower frame). All solutions start from the same initial condition $x \to k_0(\varphi)$ for $\varphi \to -\infty$. Consequently, the origin $x = 0$, $\varphi = 0$ of the coordinate system is again defined by the sheath edge of the asymptotic ($\varepsilon = 0$) solution. The sheath solutions refer again to a wall potential $\varphi_w = 3$.

For $\varepsilon = 0$, we recognize the asymptotic solution of section 3 with its singular but uniquely defined sheath edge. For all finite values $\varepsilon > 0$, however, it becomes somewhat arbitrary to define separate presheath and sheath regions, because the presheath is not completely free of space charges, and the sheath is not really collisionless. In particular, there is no distinct point separating the sheath from a quasi-neutral region, and any definition of a sheath 'edge' appears questionable.

Similar conclusions can be drawn from the ion distribution functions shown in figure 4 (see equation (11)). In the plasma region ($\varphi \lesssim -1$) the ions are rather cold, and the shape of the distribution function becomes nearly exponential [21, 23]. Approaching for $\varepsilon \ll 1$ the sheath region ($\varphi \to 0$), the increasing field and the growing inhomogeneity gain influence. The mean ion energy grows, and the distribution function at low energy $y \ll 1$ becomes small, because there are only few ions that have suffered a collision in the steep potential range $(\varphi - y, \varphi)$. Corresponding results were obtained in a numerical study for Ar ions [23].

In the limiting case $\varepsilon = 0$, the sheath edge distribution becomes zero at zero energy ($f(0, 0) = 0$) due to the field singularity $k'(0) = 0$ (see equation (11)). The sheath distribution $f(\varphi, y)$ is obtained by a parallel shift of the sheath edge distribution $f(0, y)$ (see equation (18)). Consequently,

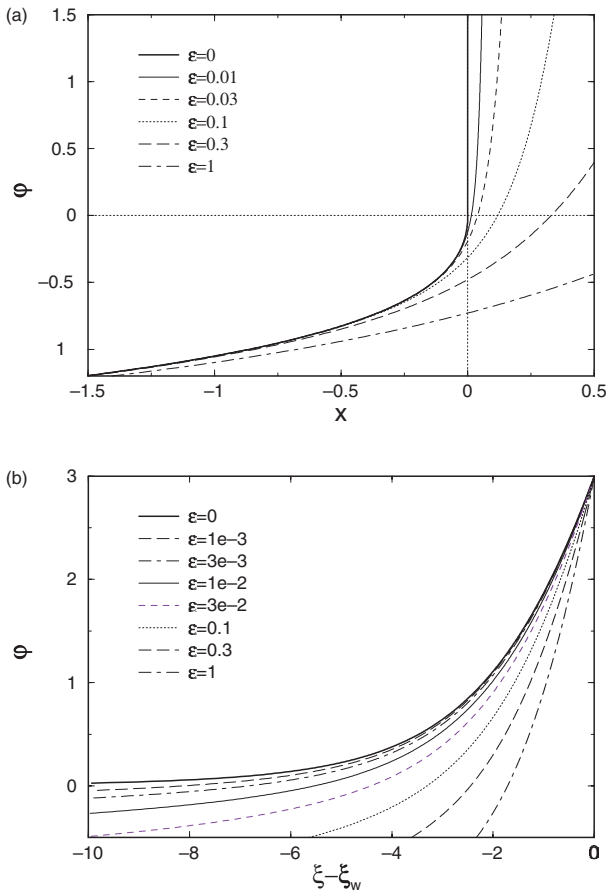

Figure 3. Potential variation in the CX boundary layer for various $\varepsilon = \lambda_D/\lambda$. Upper frame: presheath scale, $x = z/\lambda$. Lower frame: sheath scale, $\xi = z/\lambda_D$. (The sheath solutions refer to a wall potential $\varphi_w = 3$.)

the sheath is characterized by $f(\varphi, y) = 0$ for $y < \varphi$, in the presheath we have $f(\varphi, 0) > 0$, and the sheath edge is the first point, where $f(\varphi, 0) = 0$ holds. This clear distinction of the regions is trivially lost for $\varepsilon > 0$ because there are collisions in the sheath and $f(\varphi, 0) > 0$ holds both in the presheath and in the sheath. For $\varepsilon \gtrsim O(1)$, finally, the sheath becomes collision dominated, and the distribution function tends to an exponential shape everywhere [23].

From the results discussed so far we have therefore no basis to formulate convincing sheath- and presheath criteria for finite ε. As a consequence, we have seen no common representation of the plasma–sheath transition for all small but finite values of ε. This common representation, however, becomes obviously apparent in figure 5, where the same numerical solutions of figure 3 are re-plotted in the re-normalized variables

$$\varepsilon^{-8/9} x = \frac{z}{\lambda^{1/9}\lambda_D^{8/9}} \qquad \text{and} \qquad \varepsilon^{-4/9}\varphi = -\frac{\lambda^{4/9} e\Phi}{\lambda_D^{4/9}\kappa T_e} \tag{20}$$

corresponding to an intermediate scale length $\ell_m = \lambda^{1/9}\lambda_D^{8/9}$ connecting the presheath- and sheath scales.

5. Intermediate scale analysis

The numerical results of section 4 suggest investigating the plasma–sheath transition on an intermediate scale

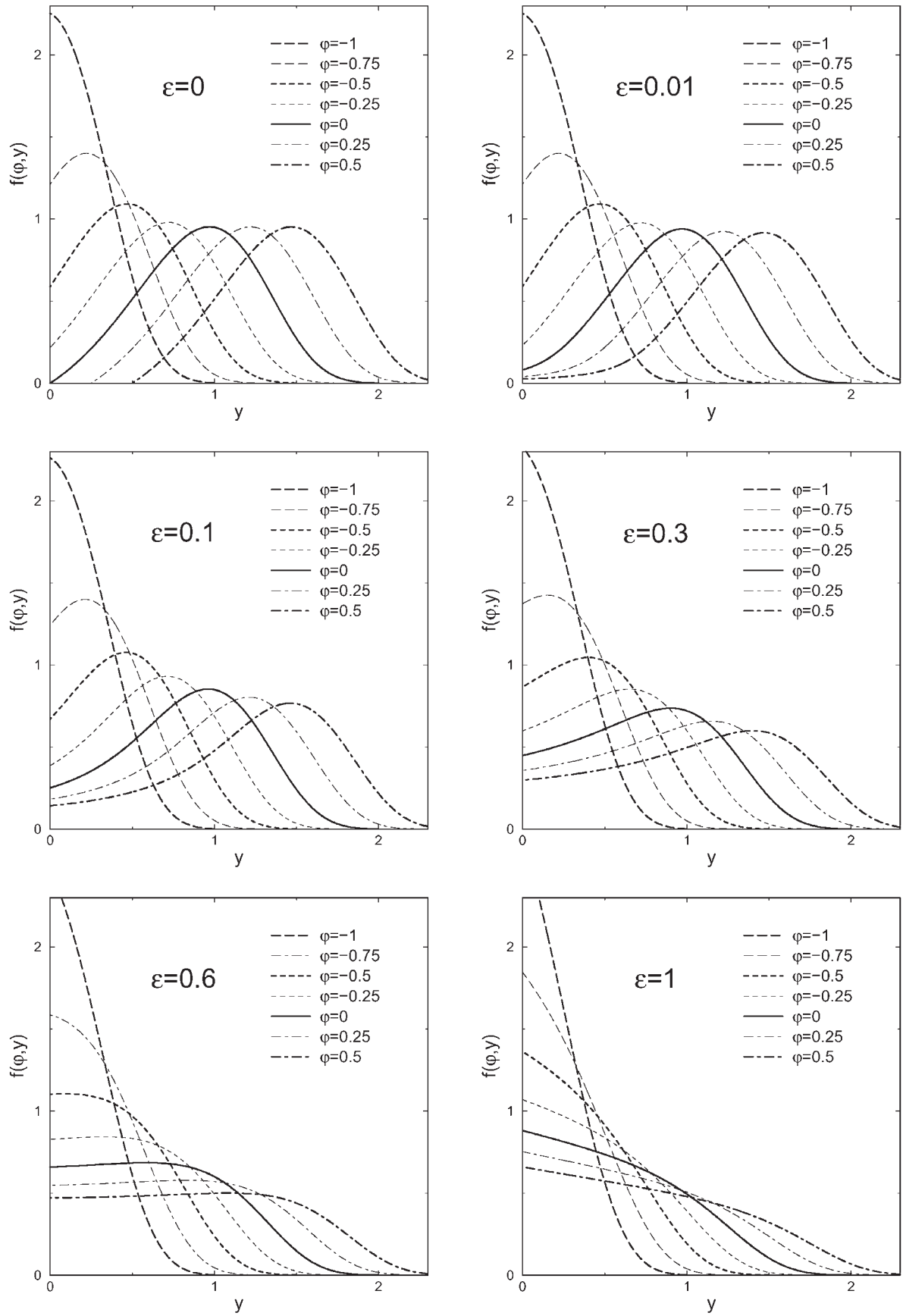

Figure 4. Ion distribution function $f(\varphi, y)$ in the CX-presheath ($\varphi < 0$) and sheath ($\varphi > 0$) for various values of $\varepsilon = \lambda_D/\lambda$.

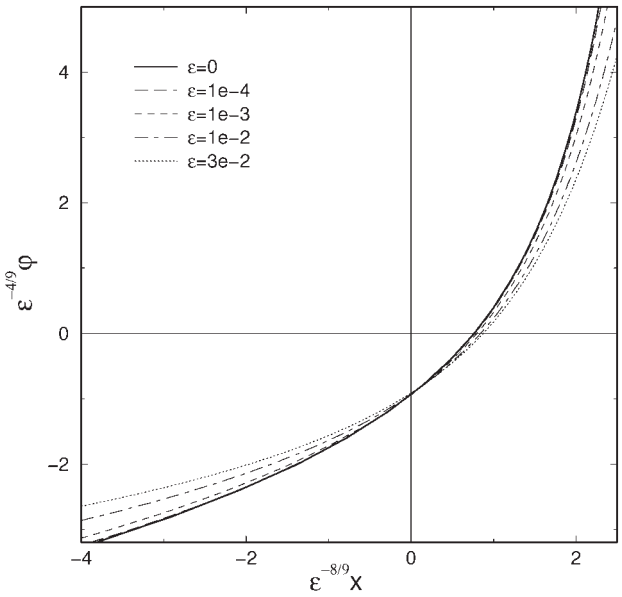

Figure 5. Variation of the re-normalized potential $\varepsilon^{-4/9}\varphi$ on the intermediate scale $\varepsilon^{-8/9}x$ for small values of $\varepsilon = \lambda_D/\lambda$.

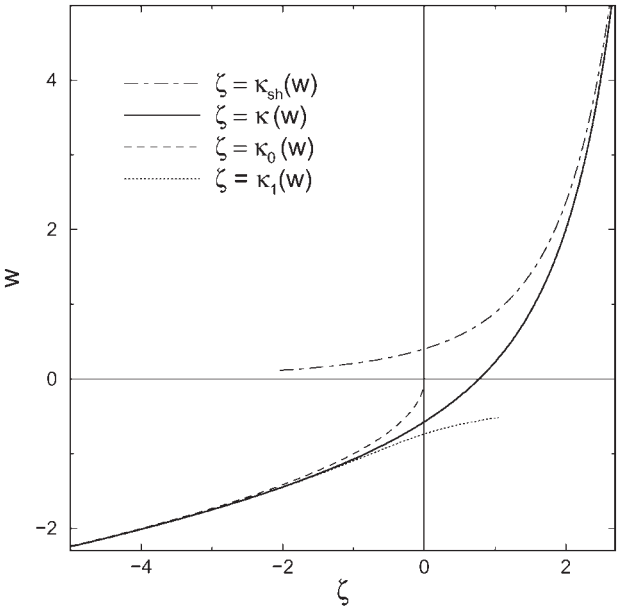

Figure 6. Asymptotic intermediate scale solution $\zeta(w)$, its sheath approximation $\kappa_{\rm sh}(w)$, and presheath expansion $\kappa_0(w)$. For $\kappa_1(w)$ see equation (27) and appendix B.

characterized by equation (20). This apparently curious scaling follows from the asymptotic solutions of section 3 by comparing the orders of magnitude of φ and x near the sheath edge. From equation (15), we have $x = \mathrm{O}(\varphi^2)$, and from equation (19) we read $x/\varepsilon = \mathrm{O}(\varphi^{-1/4})$. Equating the orders of magnitude yields $\varphi = \mathrm{O}(\varepsilon^{4/9})$ and $x = \mathrm{O}(\varepsilon^{8/9})$ in accord with equation (20).

Figure 5 presumes that there is indeed a unique intermediate scale solution for $\varepsilon = 0$. To prepare the construction of its equation let us introduce the new variables

$$w = \frac{\varphi}{\delta} \qquad \text{and} \qquad \zeta = \kappa(w) = \frac{x}{a\delta^2}$$
$$\text{with } \delta = \left(\frac{3\varepsilon^2}{8a^3 j}\right)^{2/9}. \tag{21}$$

(The numerical factors are chosen for convenience, for j and a see equations (14) and (15).) On this scale, we estimate a space charge

$$\rho = \varepsilon^2 \frac{\mathrm{d}^2\varphi}{\mathrm{d}x^2} = \mathrm{O}(\delta^{3/2}). \tag{22}$$

To connect the presheath and the sheath, we must, of course, account for this space charge. We neglect, however, terms of the order δ^2 or smaller, i.e. we aim for a zero order asymptotic theory of the intermediate scale.

At first sight it might seem that the effect of collisions on this scale was of the order $x = z/\lambda = \mathrm{O}(\delta^2)$ and could be completely neglected. This, however, is not true, because the effect of a collision consists

(a) in the loss of a fast ion ($y = \mathrm{O}(1)$) and
(b) in the gain of a slow ion ($y = \mathrm{O}(\varphi) = \mathrm{O}(\delta)$).

Since the density contribution of an ion is proportional to $y^{-1/2}$, only the collisional loss-term is correctly estimated by $\mathrm{O}(\delta^2)$ and may indeed be neglected. The gain-term, however, yields a density contribution of the order $\mathrm{O}(\delta^2\delta^{-1/2})$ competing with the space charge (see equation (22)).

To formulate this physical conclusion in a mathematical form, we start from the quasi-neutral solution $k_0(\varphi)$ to replace $\mathrm{e}^{-\varphi}$ in equation (12), and obtain

$$\varepsilon^2 \frac{\mathrm{d}^2\varphi}{\mathrm{d}x^2} = j\int_{-\infty}^{\varphi} \frac{\mathrm{e}^{k(\eta)-k(\varphi)}k'(\eta) - \mathrm{e}^{k_0(\eta)-k_0(\varphi)}k_0'(\eta)}{\sqrt{\varphi-\eta}}\mathrm{d}\eta. \tag{23}$$

Anticipating that the difference between $k(\varphi)$ and $k_0(\varphi)$ fades quickly away on the intermediate scale, there is only a small region $\sim\delta$ where we have a non-vanishing integrand. In this small region, we may omit in zeroth order the exponential factors and obtain

$$\varepsilon^2 \frac{\mathrm{d}^2\varphi}{\mathrm{d}x^2} = j\int_{-\infty}^{\varphi} \frac{k'(\eta) - k_0'(\eta)}{\sqrt{\varphi-\eta}}\mathrm{d}\eta. \tag{24}$$

Utilizing finally the representation (15) of k_0 and applying the transformation (21) we arrive at the intermediate scale equation

$$\frac{\mathrm{d}^2 w}{\mathrm{d}\zeta^2} = -\frac{\kappa''(w)}{\kappa'^3(w)} = \frac{3}{8}\int_{-\infty}^{w} \frac{\kappa'(v)+2v}{\sqrt{w-v}}\,\mathrm{d}v, \tag{25}$$

which we intended to derive. Results of a numerical solution of equation (25) are shown in figure 6 and listed in table 1, the numerical procedure is described in appendix B.

Neglecting the space charge term $\mathrm{d}^2w/\mathrm{d}\zeta^2$, we obtain the presheath approximation

$$\kappa_0(w) = -w^2 \tag{26}$$

corresponding to equation (15). First space charge corrections may be estimated from the iterated solution (see appendix B)

$$\kappa_1(w) = -w^2(1 - \tfrac{1}{4}|w|^{-9/2}). \tag{27}$$

Keeping, on the other hand, the space charge term but neglecting collisional contributions represented by the $\kappa'(v)$

Table 1. Asymptotic intermediate solution $\kappa(w)$ and its derivative $\kappa'(w)$.

w	$\kappa(w)$	$\kappa'(w)$	w	$\kappa(w)$	$\kappa'(w)$
−5	−24.995 5	10.002 2	3	2.287 36	0.237 77
−4	−15.992 2	8.004 85	4	2.491 87	0.176 44
−3	−8.984 09	6.013 07	5	2.647 76	0.138 06
−2	−3.957 74	4.049 11	10	3.101 18	0.061 32
−1	−0.832 85	2.259 53	20	3.495 46	0.026 24
0	0.772 19	1.083 79	30	3.698 26	0.015 87
1	1.558 88	0.566 33	40	3.830 51	0.011 09
2	2.001 00	0.346 24	50	3.926 83	0.008 40

and by the integration range $v < 0$ in equation (25), we obtain the sheath approximation

$$\kappa''_{\rm sh} = -\frac{3}{4}\kappa'^3_{\rm sh}\int_0^w \frac{v\,{\rm d}v}{\sqrt{w-v}} = -\frac{3}{4}\kappa'^3_{\rm sh}w^{3/2}\int_0^1 \frac{t\,{\rm d}t}{\sqrt{1-t}} = \kappa'^3_{\rm sh}w^{3/2}.$$

Integrating twice and using the sheath edge boundary condition $\kappa' \to \infty$ for $w \to 0$ we arrive at the sheath representation

$$\kappa_{\rm sh}(w) = \zeta_0 - \sqrt{20}w^{-1/4} \tag{28}$$

of the intermediate scale solution, that proves to be identical with equation (19). Comparing with the numerical solution of equation (25), we find the integration constant $\zeta_0 = 5.6084$.

Figure 6 shows the full solution $\zeta = \kappa(w)$ together with the presheath- and sheath limits $\zeta = \kappa_0(w)$ and $\zeta = \kappa_{\rm sh}(w)$. It is quite obvious that $\kappa(w)$ is indeed the 'missing link' that provides a smooth matching of the presheath- and sheath solutions for small but finite ε.

6. Generalization

Physically, the analysis of the transition region describes the first formation of space charges by the critical density contribution of slow ions. This means, as discussed, it depends on the gain-term of the Boltzmann collision integral, but not on the corresponding loss-term. Mathematically, this was expressed by the omission of the exponential factors in the transition from equation (23) to (24).

The fact, that the basic intermediate equations (24) or (25) depend only on the total production rate (expressed here by the current density j) of slow ions and not on details of the collision probability, has important consequences for the general validity of our special intermediate scale analysis. Obviously, it is valid for all 'cold' collision- and/or ionization models with arbitrary collision cross sections and ionization rates if j in equation (21) is replaced by the normalized total process rate at the sheath edge, and $a = 2k''_0(\varphi_s)$ (see equation (15)) by the sheath edge curvature of the respective presheath solution.

In particular, the analysis of section 5 is equally valid for the well known Tonks–Langmuir problem [1, 19]. It is therefore no accidental coincidence that our intermediate scale $x = {\rm O}(\varepsilon^{8/9})$ or $z = {\rm O}(\lambda_D^{8/9}L^{1/9})$ (with $L = \lambda$) is identical with the scale $\ell_m = \lambda_D^{8/9}L^{1/9}$ (with L = plasma extension) found by Franklin and Ockendon [16].

We have shown elsewhere [25] that the analysis of the generalized multi-component Tonks–Langmuir problem can be reduced to an equivalent one-component analysis. This allows one to extend the generalization even to arbitrary multi-ion systems with 'cold ion sources', i.e. to systems where the ions start with zero energy from elementary processes. We shall elaborate on this generalization in more detail in a subsequent paper.

7. Bohm criterion and sheath edge

In asymptotic analysis ($\varepsilon = \lambda_D/L = 0$) the sheath formation is closely related to the Bohm criterion, which reads in kinetic formulation [19, 3]

$$\frac{1}{m_i}\langle v_z^{-2}\rangle \leqslant \frac{1}{\kappa T_e}. \tag{29}$$

According to different arguments given by Allen [26] and Riemann [27], the sheath edge is uniquely defined by the marginal validity (equality form) of equation (29). This equality form may be utilized to formulate the boundary conditions of a kinetic plasma analysis [28,29]. It is therefore both a problem of principle and a task of practical interest to investigate the significance of the Bohm criterion for finite ε.

In our notation equation (29) reads

$$\frac{1}{2n}\int_0^\infty y^{-3/2}f(\varphi, y)\,{\rm d}y \leqslant 1. \tag{30}$$

Obviously, the integral depends extremely delicately on the contribution of slow ions ($y \to 0$), and the very existence of the integral requires that the ion distribution function vanishes at zero energy, $f(\varphi, 0) = 0$. Inspecting the ion distribution functions presented in figure 4, we see that this trivial condition is fulfilled exclusively in the asymptotic case ($\varepsilon = 0$) and then exclusively in the sheath region ($\varphi \geqslant 0$). For arbitrarily small but finite values of ε the integral exists nowhere and, consequently, the Bohm criterion (30) can not give any information on the sheath formation for finite ε.

We may try to overcome this difficulty by a mathematical trick. Integrating by parts, we obtain from equation (30)

$$B(\varphi) = \frac{1}{n}\int_0^\infty y^{-1/2}\frac{\partial f(\varphi, y)}{\partial y}\,{\rm d}y \leqslant 1. \tag{31}$$

Whenever the integral in equation (30) exists, equations (30) and (31) are equivalent. Consequently, it appears self-suggesting to re-formulate the kinetic Bohm criterion in the form $B(\varphi) \leqslant 1$ which is defined for arbitrary values of ε and φ.

$B(\varphi)$ may be calculated from equation (31) by numerical integration. It is, however, more elucidating to investigate it directly from Boltzmann's equation. Multiplying equation (9) with $y^{-1/2}$ and integrating over all positive energies $y > 0$ yields

$$nB(\varphi) + \frac{{\rm d}n}{{\rm d}\varphi} = -nk'(\varphi). \tag{32}$$

Considering first the asymptotic case $\varepsilon = 0$, we have $k' = 0$ in the sheath ($\varphi > 0$) and $k' = k'_0$, $n = {\rm e}^{-\varphi}$ in the presheath ($\varphi < 0$), or

$$B_0(\varphi) = \begin{cases} -\dfrac{1}{n}\dfrac{{\rm d}n}{{\rm d}\varphi} & (\varphi > 0), \\ 1 - k'_0(\varphi) & (\varphi \leqslant 0). \end{cases} \tag{33}$$

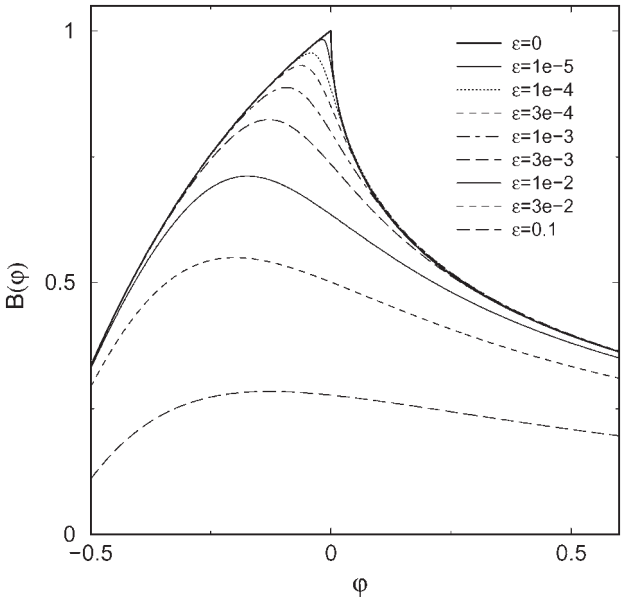

Figure 7. Variation of the Bohm integral $B(\varphi)$ (see equations (31) and (32)) for various values of $\varepsilon = \lambda_D/\lambda$.

This shows that the sheath edge singularity $k_0'(0) = 0$ confirms indeed the marginal value $B_0 = 1$ at the sheath edge. The presumed 'sheath condition' $B_0 < 1$, however, is fulfilled both in the sheath ($|\mathrm{d}n/\mathrm{d}\varphi| < n$) and in the presheath ($k_0' > 0$). Consequently, there is no sheath information in the value of B_0, except for the one point with $B_0 = 1$ characterizing the sheath edge!

For finite values $\varepsilon > 0$, the potential profiles become flatter, and both arguments $|\mathrm{d}n/\mathrm{d}\varphi| < n$ and $k' > 0$ hold in the sheath and in the presheath as well. Consequently, the inequality $B \leqslant 1$ is fulfilled always and everywhere and is no indicator for anything. These results are confirmed by the numerical calculations presented in figure 7. (From the figure one might suspect that the plasma–sheath transition is generally related to a maximum of $B(\varphi)$. This vague conjecture, however, will be disproved with the results of a subsequent paper investigating other presheath mechanisms.)

We must therefore conclude that the Bohm criterion is significant exclusively in the asymptotic case $\varepsilon = 0$, and then only in its marginal form which is uniquely related to the sheath edge. For finite values of ε, the onset of space charge formation becomes fuzzy, and the Bohm criterion loses its significance. This confirms and intensifies former conclusions from fluid theory [18].

8. Summary and discussion

The usual subdivision of the plasma boundary layer into a quasi-neutral presheath (typical extension L) and a collision-free sheath (typical extension λ_D) is based on a small ratio $\varepsilon = \lambda_D/L$ and strictly valid only in the asymptotic limit $\varepsilon = 0$. The interface connecting presheath and sheath, the sheath edge, is closely related to the equality form of the Bohm criterion and characterized by a mathematical singularity. This singularity prevents a smooth matching of the presheath- and sheath solutions and has given rise to numerous controversies.

In this paper, we have investigated the boundary layer of a collision dominated plasma ($L = \lambda$) kinetically on the basis of the cold CX model of [21]. In the asymptotic limit $\varepsilon = 0$, this model exhibits clearly the unique definition of the sheath edge and its relation to the equality form of the (kinetic) Bohm criterion. For finite values of ε, however, the onset of space charge formation becomes fuzzy, and the Bohm criterion loses its significance.

Nevertheless there is a uniquely defined transition region, the intermediate scale, replacing the sheath edge for small but finite values of ε. This transition region follows free of arbitrariness from the asymptotic theory. Physically, it is characterized by the first space charge formation due to slow ions generated in CX collisions. The transition region has a typical extension $\ell_m = \lambda_D^{8/9}\lambda^{1/9}$, and the intermediate scale analysis is characterized by the transformation (21) and the parameter free basic equation (25). Its solution determines the self-consistent potential and is listed in table 1. Figure 6 demonstrates that it is indeed the missing link that enables a smooth matching of the presheath- and sheath solutions.

Actually, the intermediate scale resolves the asymptotic sheath edge and removes all difficulties with the sheath edge singularity due to a more detailed description of the space charge formation. Its extension ℓ_m is large compared with the Debye length and small compared with the mean free path, thus confirming the asymptotic sheath- and presheath representations

$$\xi_s \sim -\frac{\ell_m}{\lambda_D} \to -\infty \qquad \text{and} \qquad x_s \sim -\frac{\ell_m}{\lambda} \to 0 \quad (34)$$

of the sheath edge position. From the transformations (21) and from $\mathrm{d}w/\mathrm{d}\zeta = \mathrm{O}(1)$ we conclude further that the transition region is distinguished by an electric field

$$E_s \sim \frac{kT_e}{e\lambda^{5/9}\lambda_D^{4/9}}. \quad (35)$$

This finite value represents the actual sheath edge field and explains the asymptotic ($\lambda_D/\lambda \to 0$) sheath- and presheath representations

$$\left.\frac{\mathrm{d}\varphi}{\mathrm{d}\xi}\right|_{\xi_s} = \frac{eE_s\lambda_D}{kT_e} \sim \varepsilon^{5/9} \to 0, \qquad \left.\frac{\mathrm{d}\varphi}{\mathrm{d}x}\right|_{x_s} = \frac{eE_s\lambda}{kT_e} \sim \varepsilon^{-4/9} \to \infty, \quad (36)$$

which are frequently mis-interpreted.

In section 6, we have given arguments showing that the intermediate scale analysis presented here is not restricted to the CX model. We shall elaborate on this in a subsequent paper, but we anticipate that the intermediate scale solution is universal for all 'cold' kinetic models, i.e. for interaction models where the ions start at rest from elementary processes. A corresponding universality exists neither for the presheath- nor for the sheath solution.

The reference to 'cold' kinetic models is important due to the decisive density contribution of slow ions. Since this critical contribution cannot be described in the frame of an average velocity attributed to all ions, fluid models result in a different scaling $\ell_m = \lambda_D^{4/5}L^{1/5}$ of the transition layer.

A different scaling must also be expected for 'hot' kinetic models where the ions emerge from elementary processes with an energy that is comparable to the thermal electron energy. A corresponding analysis is apparently not available, but there are reasons to predict a scaling $\ell_m = \lambda_D^{6/7} L^{1/7}$ [3,4].

Appendix A. Numerical solution of the plasma–sheath equation

The solution of equation (12) starts with an approximation of 'weak inhomogeneity' in the plasma region $\varphi \lesssim -2$. Assuming that the electric field φ' is nearly constant over a mean free path, we calculate

$$\int_{-\infty}^{\varphi} \frac{\mathrm{e}^{k(\eta)} k'(\eta)\,\mathrm{d}\eta}{\sqrt{\varphi-\eta}} \approx \varphi'^{-1/2} \int_{-\infty}^{x} \frac{\mathrm{e}^{x'}\,\mathrm{d}x'}{\sqrt{x-x'}} = \sqrt{\frac{\pi}{\varphi'}}\mathrm{e}^{x} = \sqrt{\pi k'(\varphi)}\mathrm{e}^{k(\varphi)}$$

and obtain the differential equation

$$\sqrt{\pi j^2 k'(\varphi)} = \mathrm{e}^{-\varphi} - \varepsilon^2 \frac{k''(\varphi)}{k'^3(\varphi)}.$$

In the plasma region, the space charge term yields only a small correction. Calculating this correction by one iteration step we arrive at the approximation

$$k_1'(\varphi) = \frac{\mathrm{e}^{-2\varphi}}{\pi j^2}(1 + 4\varepsilon^2\pi^2 j^4 \mathrm{e}^{5\varphi}). \tag{37}$$

To prepare the numerical integration in the inhomogeneous presheath we choose a starting value φ_0 in the range of validity of equation (37), introduce the notations

$$\begin{aligned} \psi &= \varphi - \varphi_0, & \chi &= \eta - \varphi_0, \\ k_0 &= k(\varphi_0), & Y(\psi) &= \mathrm{e}^{k(\varphi)-k_0} \end{aligned} \tag{38}$$

and obtain equation (12) in the form

$$j\int_0^{\psi} \frac{Y'(\chi)\,\mathrm{d}\chi}{\sqrt{\psi-\chi}} = Y(\psi)\left(\mathrm{e}^{-\varphi} - \varepsilon^2\frac{k''(\varphi)}{k'^3(\varphi)}\right) - jR(\varphi,\varphi_0)$$
$$\text{with } R = \mathrm{e}^{-k_0}\int_{-\infty}^{\varphi_0} \frac{\mathrm{e}^{k(\eta)}k'(\eta)\,\mathrm{d}\eta}{\sqrt{\varphi-\eta}}. \tag{39}$$

To evaluate the remaining integral R we may again engage the approximation of weak inhomogeneity and obtain

$$R(\psi,\varphi_0) = \sqrt{\pi k'(0)}\mathrm{e}^{k'(\varphi_0)\psi}\mathrm{erfc}(\sqrt{k_0'(\varphi_0)\psi}). \tag{40}$$

Corresponding to the homogeneity of the problem, k_0 is a free integration constant which does not appear in the basic equations (39) and (40). We fix k_0 by choosing the sheath edge position $x = 0$ for $\varepsilon = 0$. (Choosing $\varphi_0 = -2$ this results in $k_0 = -10.050\,292$, i.e. the starting point of the numerical integration has a distance of about ten mean free paths from the sheath edge.)

To solve equation (39) numerically, we use an equidistant grid $\psi_\nu = \nu h$ and use the abbreviations

$$\begin{aligned} Y_\nu &= Y(\psi_\nu), & Y_\nu' &= Y'(\psi_\nu), \\ k_\nu &= k(\varphi_0+\psi_\nu), & k_\nu' &= k'(\varphi_0+\psi_\nu). \end{aligned} \tag{41}$$

The integral in equation (39) is evaluated with the approximation

$$\int_0^{\psi_n} \frac{Y'(\chi)\,\mathrm{d}\chi}{\sqrt{\psi-\chi}} = \frac{2}{3}h^{1/2}n^{1/2}[2nY_1' + (3-2n)Y_0']$$
$$+\frac{4}{3}h^{1/2}\sum_{\nu=1}^{n-1}(n-\nu)^{3/2}(Y_{\nu-1}' - 2Y_\nu' + Y_{\nu+1}'), \tag{42}$$

which is exact for stepwise linear functions Y'. To calculate the space charge term k''/k'^3 on the right-hand side we use

$$k_n' = \frac{Y_n'}{Y_n} \qquad \text{and} \qquad k_n'' = \frac{(3/2)k_n' - 2k_{n-1}' + (1/2)k_{n-2}'}{h}. \tag{43}$$

Relating finally Y and Y' by Simpson's formula

$$Y_n = Y_{n-2} + \frac{h}{3}(Y_{n-2}' + 4Y_{n-1}' + Y_n') \tag{44}$$

and starting with initial conditions ($\nu = 0, 1$) calculated from equation (37), the entire scheme can be solved successively for Y_n'.

Appendix B. Numerical solution of the intermediate scale equation

Since the structure of equation (25) is similar to that of equation (12), we can use a similar solution scheme. The main difference consists in the plasma-sided starting conditions, where the approximation $k_1(\varphi)$ of weak inhomogeneity must be replaced by a suitable approximation $\kappa(w) = \kappa_1(w)$ for $w \leqslant w_0$. To find κ_1, we improve the presheath approximation $\kappa_0(w) = -w^2$ (see equation (26)) by one iteration step and obtain from equation (25)

$$\frac{3}{8}\int_{-\infty}^{w} \frac{\kappa_1'(v)+2v}{\sqrt{w-v}}\mathrm{d}v = -\frac{\kappa_0''(w)}{\kappa_0'^3(w)} = \frac{-1}{4w^3}. \tag{45}$$

Equation (45) is an Abel type integral equation for κ_1' that can be solved analytically, we find

$$\begin{aligned} \kappa_1'(w) &= -2w + \tfrac{5}{8}(-w)^{-7/2}, \\ \kappa_1(w) &= -w^2 + \tfrac{1}{4}(-w)^{-5/2}. \end{aligned} \tag{46}$$

Inspecting figure 6 and table 1, we see that $\kappa_1(w)$ converges very rapidly to the exact solution $\kappa(w)$. Choosing a starting value $w_0 \lesssim -5$, we can identify κ' and κ_1' for $w \leqslant w_0$ and obtain from equation (25)

$$\int_{w_0}^{w} \frac{\kappa'(v)+2v}{\sqrt{w-v}}\mathrm{d}v + \tilde{R} = -\frac{8}{3}\frac{\kappa''}{\kappa'^3}$$
$$\text{with } \tilde{R} = \int_{-\infty}^{w_0} \frac{\kappa_1'(v)+2v}{\sqrt{w-v}}\mathrm{d}v. \tag{47}$$

The remaining integral r is elementary, but the vicinity of $w = 0$ is better represented by a series expansion. We obtain

$$\tilde{R}(w,w_0) = \begin{cases} \dfrac{1}{3w^3}\left[\sqrt{\dfrac{w-w_0}{-w_0}}\left(2 + \dfrac{w}{w_0} + \dfrac{3w^2}{4w_0^2}\right) - 2\right] \\ \quad (w \neq 0), \\ \dfrac{-5}{8w_0^3}\left(\dfrac{1}{3} + \dfrac{w}{8w_0} + \dfrac{3w^2}{40w_0^2} + \dfrac{5w^3}{96w_0^3}\right) \\ \quad (|w| \ll |w_0|). \end{cases} \tag{48}$$

Introducing finally the notation

$$\begin{aligned} u &= w - w_0, \qquad & x &= v - w_0, \\ y(u) &= \kappa(w_0 + u), \qquad & y'(u) &= \kappa'(w_0 + u), \end{aligned} \tag{49}$$

we obtain from equation (47)

$$\int_0^u \frac{y'(x)\,\mathrm{d}x}{\sqrt{u-x}} = -4u^{1/2}\left(w_0 + \frac{2}{3}u\right) - \frac{8}{3}\frac{y''}{y'^3} - \tilde{R}. \tag{50}$$

This equation has the same structure as equation (39) and is solved according to the same numerical scheme.

References

[1] Tonks L and Langmuir I 1929 *Phys. Rev.* **34** 876
[2] Bohm D 1949 *The Characteristics of Electrical Discharges in Magnetic Fields* ed A Guthrie and R Wakerling (New York: McGraw-Hill) chapter 3
[3] Riemann K-U 1991 *J. Phys. D: Appl. Phys.* **24** 493
[4] Riemann K-U 2000 *J. Techn. Phys.* **41** 99 (*Gen. Inv. Lect. XXIVth ICPIG (Warsaw, 1999)*)
[5] Stangeby P C and Allen J E 1970 *J. Phys. A: Gen. Phys.* **3** 304
[6] Hall L S 1962 *Proc. Phys. Soc.* **80** 309
[7] Godyak A V 1982 *Phys. Lett.* **89A** 80
[8] Godyak A V and Sternberg N 1990 *IEEE Trans. Plasma Sci.* **18** 159
[9] Zawaideh E, Kim N S and Najmabadi F 1990 *Phys. Fluids* B **2** 647
[10] Valentini H B 1996 *Phys. Plasmas* **3** 1459
[11] Godyak A V and Sternberg N 2002 *Phys. Plasmas* **9** 4427
[12] Riemann K-U and van den Berg H-P 1991 *Phys. Fluids* B **3** 1300
[13] Riemann K-U and Meyer P 1996 *Phys. Plasmas* **3** 4751
[14] Su C H 1967 *Proc. 8th Int. Conf. on Phenomena in Ionized Gases (Vienna, 1967)* vol I (Vienna: IAEA) p 569
[15] Lam S H 1965 *Phys. Fluids* **8** 73
Lam S H 1965 *Proc. 8th Int. Conf. on Phenomena in Ionized Gases (Vienna, 1967)* vol I (Vienna: IAEA) p 545
[16] Franklin R N and Ockendon J R 1970 *J. Plasma Phys.* **4** 371
[17] Kaganovich I D 2002 *Phys. Plasmas* **9** 4788
[18] Riemann K-U 1997 *Phys. Plasmas* **4** 4158
[19] Harrison E R and Thompson W B 1959 *Proc. Phys. Soc.* **74** 145
[20] Riemann K-U 1978 *J. Nucl. Mater.* **76&77** 575
Riemann K-U 1979 *J. Physique Coll.* **40** 831
[21] Riemann K-U 1981 *Phys. Fluids* **24** 2163
[22] Holstein T 1952 *J. Phys. Chem.* **56** 832
[23] Vasenkov A V and Shizgal B D 2002 *Phys. Rev.* E **65** 046404-1
[24] Vasenkov A V and Shizgal B D 2002 *Phys. Plasmas* **9** 691
[25] Riemann K-U 2003 *J. Phys. D: Appl. Phys.* **36**
[26] Allen J E 1976 *J. Phys. D: Appl. Phys.* **9** 2331
[27] Riemann K-U 1980 *Proc. Int. Conf. on Plasma Physics (Nagoya)* vol I, p 66
Riemann K-U 1989 *Phys. Fluids* B **1** 961
[28] Bissel R C and Johnson P C 1987 *Phys. Fluids* **30** 779
[29] Bissel R C 1987 *Phys. Fluids* **30** 2264